Tomography of Turbulence Strength Based on Scintillation Imaging
Supplementary Material

Nir Shaul and Yoav Y. Schechner

Viterbi Faculty of Electrical and Computers Eng.,
Technion - Israel Institute of Technology, Haifa, Israel
nir.shaul@gmail.com , yoav@ee.technion.ac.il

Abstract. This is a supplementary document to the main manuscript. This document provides a detailed theoretical explanation and an illustration of the *seeing* effect, as a comparison to the scintillation effect. We also attach a video sample of the acquired data from the field experiment conducted in 02/02/2022. Additionally, we provide more simulated results.

1 Outline

This supplementary document contains four sections. Sec. 2 gives another intuition for the phenomenon of *seeing* and its path integral characteristics. In Sec. 3, we explain the scenario in the attached video, sampled during the outdoor experiment. Sec. 4 provides additional results of the simulated scintillation formation signal.

2 Modeling the Seeing Effect

According to Sec. 2 of the main manuscript, one of the turbulence visual effects is termed *seeing*. In this effect, random refraction perturbs the angle of arrival (AOA) of a ray from an object to the camera. Thus, the LOS of each pixel wiggles, creating spatiotemporal geometric distortions in image sequences. For an object at distance L and a camera having a lens aperture diameter D, the AOA of a line of sight (LOS) has variance given by Eqs. (3,4) of the main manuscript. The contribution is maximal by a turbulent air parcel right near the camera lens.

Here we provide an intuitive illustration of how a turbulent medium creates seeing, in a pinhole camera observing a single isotropic point source. Consider a very simplified case, where an air parcel has a shape of a prism, and its refractive index is slightly higher than that of calm steady air. Then, the air parcel acts as a refracting medium (Fig.1 herein). This effect yields a first order perturbation of the AOA.

If the air parcel is adjacent to the isotropic point source ($z = 0$), then it has a negligible effect on the AOA at the camera. As a result, no matter what is the

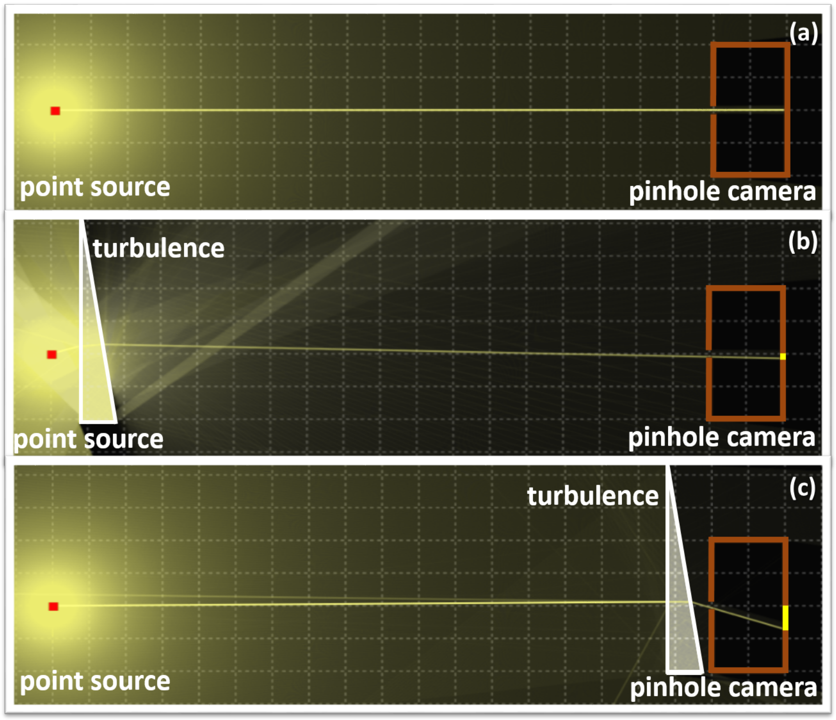

Fig. 1. Ray tracing simulation, illustrating the turbulence *seeing* phenomenon using a thin prism and a pinhole camera. The turbulence AOA influence is minor, when the turbulence is located close to the source (**b**). The influence becomes major when the turbulence is located near the camera pinhole (**c**). Based on the ray-tracing simulator of [1].

random refractive index of the air parcel, it does not change the AOA in this case. However, if the air parcel is adjacent to the pinhole camera, $(z = L)$, it has a significant effect: the light ray which enters the pinhole can have a high AOA bias. Because the air-parcel has a random refractive index, the perturbation of the AOA is random, and in this case, having high values of σ^2_{AOA}. This leads to observed seeing.

3 Scintillating Lights Capturing

We make the the raw data, codes and system design of the field experiment publicly available in: `https://github.com/nirshaul/ScintillationTomography` We also attach a video sampled during the outdoor experiment. The video file includes 50 frames of scintillating lights in the scene, as captured in viewpoint 4. The video attached is a compressed version (95%, for file upload limits) of the operational capture. In Fig. 2 herein, we can notice the same scene of the operational video, as captured in the preliminary capture. In this scene we can

Fig. 2. Preliminary capture of the scene in the attached video file. Taken from viewpoint 4, angle 20.

notice a complex urban region composed of an industrial foreground, rural and residential background areas. Notice the strong scintillation of lights in the upper part of the image (background), where LOSs, cross through the industrial area.

4 Model Simulation

The scintillation model described in Sec. 3 of the main paper is influenced by multiple imaging parameters. In this section we show how some imaging parameters influence the scintillation signal, in terms of the scintillation index estimation relative error:

$$\epsilon_{\text{err}} = \frac{|\hat{\sigma}_I^2 - \sigma_I^2|}{\sigma_I^2}. \tag{1}$$

Settings as mentioned in Sec. 5 of the main manuscript are used here. Each pixel has full-well of 3000 photoelectrons and 8-bit quantization, ie., the expected number of photoelectrons per graylevel is 11.8. Using these specifications, each noisy measurement is drawn from a Poisson distribution of photoelectrons, and then quantized. A sequence of 1000 frames was used for analysis. From this sequence, we estimated $\hat{\sigma}^2_{\mathrm{I}\bullet}$. We used a spatial gaussian (a kernel of 50×50 pixels, having standard deviation $\sigma_{\mathrm{g}} = 5$ pixels), as a captured light source, i.e.

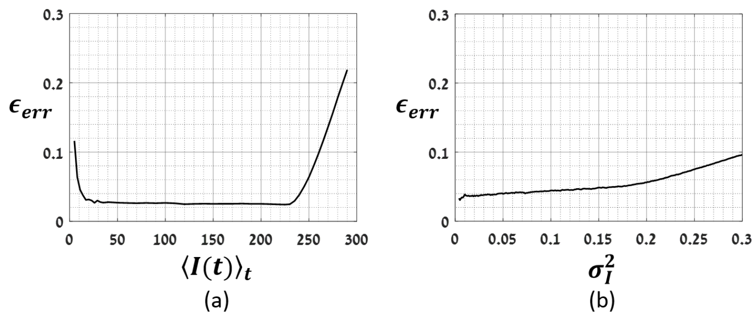

Fig. 3. (a) $\epsilon_{\rm err}$ as function of $\langle I(t) \rangle_t$ **(b)** $\epsilon_{\rm err}$ as function of $\sigma_{\rm I}^2$.

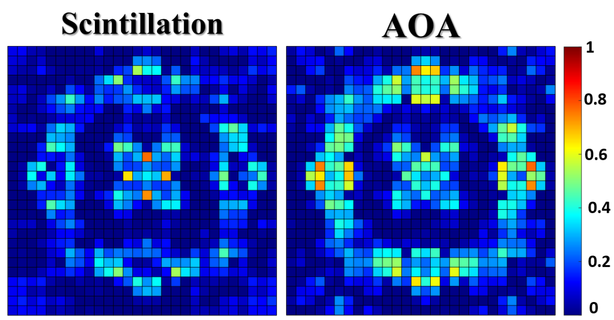

Fig. 4. Ratio of TS Reconstruction error relative to to the ground truth, by scintillation (left) and by AOA (right).

a blob in an image. We compensated the photon noise variance according to Eq.(12) of the main manuscript.

We studied how varying $\sigma_{\rm I}^2$ between 0.001 to 0.3 (typical values for very weak to weak scintillation) affect the estimation results (Fig. 3b herein). We can see that $\epsilon_{\rm err}$ increases with the scintillation index.

In addition, we studied how the temporal mean value of a scintillating blob, i.e. $\langle I(t) \rangle_t$, affects $\epsilon_{\rm err}$ (Fig. 3a herein). As expected, for high values of $\langle I(t) \rangle_t$, the signal clips due to saturation of the sensor. So, the estimation degrades (high $\epsilon_{\rm err}$). On the other hand, in low values of $\langle I(t) \rangle_t$, the acquisition suffers from a low signal to noise ratio, which also degrades the estimation.

We also studied how $\sigma_{\rm g}$ (spatial standard deviation of the captured source) affects $\epsilon_{\rm err}$. We examined the range $0.5 \le \sigma_{\rm g} \le 30$, and noticed that this parameter has no influence on $\epsilon_{\rm err}$.

In Fig. 4 herein, we add an additional visualization of the simulated experiment of Fig. 6 of the main manuscript. The figure shows the ratio of the turbulence-strength (TS) error, to the ground-truth. Notice the error is major in AOA reconstruction.

References

1. Yi-Ting Tu, J.: Ray Optics Simulation. `ricktu288.github.io/ray-optics/`